Journal of Organometallic Chemistry 825-826 (2016) 33–40

Contents lists available at ScienceDirect

Journal of Organometallic Chemistry

journal homepage: www.elsevier.com/locate/jorganchem

Synthesis, photo- and electro-luminescence of red-emitting Ir(III) complexes with 2-(1-naphthyl)benzothiazole and carrier transporting group-functionalized picolinate ligands

Tianzhi Yu [a, *], Yanjun Bao [a], Yuling Zhao [b], Hui Zhang [a], Zixuan Xu [a], Xiaomeng Wu [c]

[a] Key Laboratory of Opto-Electronic Technology and Intelligent Control (Ministry of Education), Lanzhou Jiaotong University, Lanzhou 730070, China
[b] School of Chemical and Biological Engineering, Lanzhou Jiaotong University, Lanzhou 730070, China
[c] School of Materials Science and Engineering, Southwest Jiaotong University, Sichuan 611756, China

ARTICLE INFO

Article history:
Received 20 August 2016
Received in revised form
14 October 2016
Accepted 15 October 2016
Available online 15 October 2016

Keywords:
Iridium(III) complex
2-(1-Naphthyl)benzothiazole
Photoluminescence
Electroluminescence

ABSTRACT

Two new red-emitting Ir(III) complexes containing 2-(1-naphthyl)benzothiazole as cyclometalated ligands and the carrier transporting group-functionalized picolinate as ancillary ligands have been successfully synthesized and characterized. The Ir(III) complexes have good thermal stability with less than 2% weight-reduction occurring at 285 °C, and exhibit strong red emissions. The doped light-emitting devices using the Ir(III) complexes as dopants were fabricated. The result indicated that the light-emitting devices fabricated by the carbazole-functionalized complex and the diaryl-1,3,4-oxadiazole-functionalized complex exhibited red emissions with a maximum brightness of 3074 and 2520 cd/m^2 at 10.7 V and a maximum current efficiency of 4.84 and 5.18 cd/A, respectively.

1. Introduction

In the past decades, organic light-emitting diodes (OLEDs) have attracted tremendous interest in the field of full-color display due to the potential advantages. Phosphorescent materials caused considerable attentions because of their excellent luminescent properties such as harvesting singlet and triplet excitons through the strong spin–orbit coupling of heavy metal ions (Os, Ir, Pt, Re) with d^6 and d^8 electronic structure, and enabling the internal quantum efficiencies approaching 100% [1–3]. Therefore, phosphorescent materials and devices have been intensively studied because of their high efficiencies [4–7]. Of the transition metal complexes, the cyclometalated iridium(III) complexes are widely investigated due to their relatively short excited-state lifetime, high quantum efficiency and excellent color diversity. The variable emission from the Ir(III) complexes can be tuned from the blue light to the near-IR light through the design and synthesis of novel cyclometalating and ancillary ligands [8–13].

Benzothiazole and their derivatives is a very important class of five-membered heterocyclic compounds. Benzothiazole derivatives were widely used for the synthesis of some organic photoelectric materials, such as liquid crystal materials [14], non-linear optical materials [15,16], fluorescent chromophores [17–19], and the metal complexes used in OLEDs [20–24]. Furthermore, benzothiazole derivatives have been used for organic photovoltaics as well [25–27]. Wang et al. [20] reported a series of orange-emitting Ir(III) complexes containing the 2-phenylbenzothiazole derivatives and highly efficient orange OLEDs, in which the orange OLEDs fabricated from tris(2-phenylbenzothiazolate-N,C$^{2'}$)iridium had a brightness of 95800 cd/m^2 and a maximum luminance efficiency of 87.9 cd/A (46.0 lm/W). For the derivatives of bis(2-phenylbenzothiazolate-N,C$^{2'}$)iridium(acetylacetone) [(bt)$_2$Ir(acac)], they also demonstrated that the introduction of an electron-withdrawing substituent in the 6-position of the benzothiazole ring resulted in a dramatic ascent of the orange OLEDs performances for the orange-emitting iridium(III) complexes. By introducing a strong electron-withdrawing CF$_3$ in the 6-position of the benzothiazole ring of 2-phenylbenzothiazole ligand, the orange OLEDs exhibited a maximum luminance efficiency of 76 cd/A and a brightness of 80190 cd/m^2, respectively.

Both the electroluminescent efficiency and the emissive

---

* Corresponding author.
E-mail address: yutianzhi@hotmail.com (T. Yu).

http://dx.doi.org/10.1016/j.jorganchem.2016.10.027
0022-328X/© 2016 Elsevier B.V. All rights reserved.

wavelength of the devices based on iridium(III) complexes are affected greatly by the cyclometalating and ancillary ligands [28]. Although 2-phenylbenzothiazole is one typical ligand framework to construct orange iridium(III) complexes, the conjugation of 2-phenylbenzothiazole framework is increased, which can lead to red-shifted emission of their Ir(III) complexes. In addition, the carbazole and oxadiazole derivatives have excellent solubility, stability and excellent carrier transporting characteristics, they have been widely utilized as organic optoelectronic materials. In order to improve the carrier transporting property of the emitting Ir(III) complexes, the oxadiazole or carbazole groups were usually grafted to the Ir(III) complexes [29,30].

In this work, we used 2-(1-naphthyl)benzothiazole as cyclometalated ligands and the carrier transporting group-functionalized picolinate as ancillary ligands to synthesize two new Ir(III) complexes. The experimental results reveal that the Ir(III) complexes exhibit red emissive colors. The photophysical properties and thermal stability of these complexes were investigated. Furthermore, the red-emitting OLEDs containing these complexes as dopant emitters were fabricated to investigate the electroluminescence properties of the complexes.

The synthetic routes of the Ir(III) complexes were shown in Scheme 1.

2. Experimental

2.1. Materials and methods

2-Aminothiophenol and 1-naphthaldehyde were bought from Alfa Aesar. Carbazole and sodium borohydride were obtained from Shanghai Zhongqin chemical reagent Co. Ltd. *p*-Bromobenzaldehyde was bought from Aladdin Chemistry Co., Ltd. Tri-*tert*-butylphosphine was purchased from Puyang Huicheng Electronic Materials Co., Ltd. $IrCl_3 \cdot nH_2O$ (iridium content > 60.0%) was bought from Shanxi Kaida Chemical Co. Ltd. (China) and used without further purification. 3-hydroxypicolinic acid was obtained from TCI Shanghai (China). 8-Hydroxyquinolinolato-lithium (Liq), 1,3,5-Tri(*N*-phenylbenzimidazol-2-yl)benzene (TPBi), 4,4′-Bis(9-carbazolyl)biphenyl (CBP) and 4,4′-cyclohexylidenebis(*N*,*N*-bis(p-tolyl)aniline) (TAPC) were purchased from Electro-Light Technology Corp., Beijing. All other chemicals were analytical grade reagent.

The intermediates, 9-(4-(bromomethyl)phenyl)-9*H*-carbazole and 2-[4-(Bromomethyl)phenyl]-5-(4-tertbutylphenyl)-1,3,4-oxadiazole were prepared as previously described [31,32], respectively.

^{1}H NMR spectra were obtained on Varian Mercury Plus 400 MHz. Mass spectrum was obtained from a Thermo Scientific

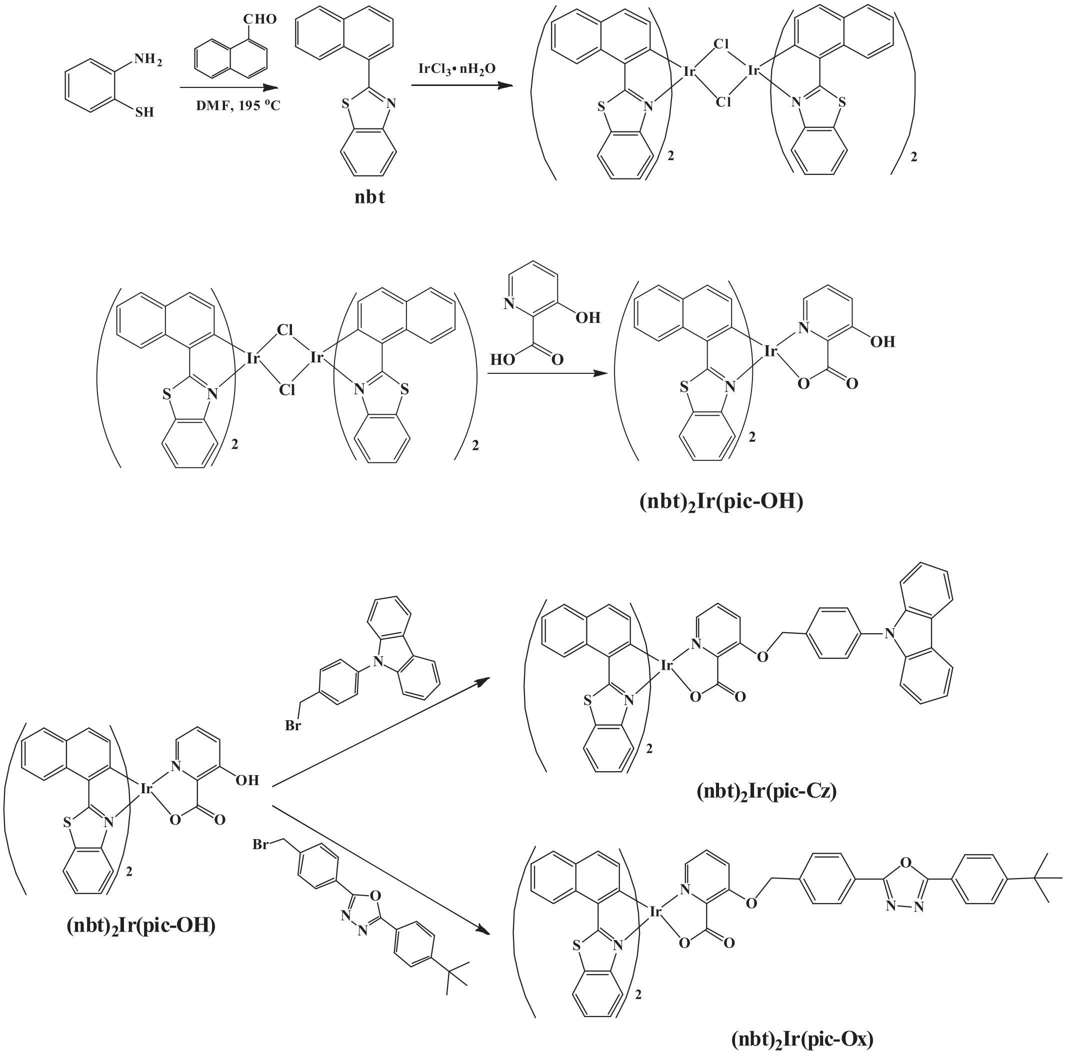

Scheme 1. Synthetic routes of the ligands and the Ir(III) complexes.

Orbitrap Elite mass spectrometer. Thermogravimetric analysis (TGA) was performed on a Perkin-Elmer Pyris system. UV–vis absorption and photoluminescent spectra were recorded on a Shimadzu UV-2550 spectrometer and on a Perkin-Elmer LS-55 spectrometer, respectively. Melting points were measured by using an X-4 microscopic melting point apparatus made in Beijing Taike Instrument Limited Company, and the thermometer was uncorrected.

2.2. Synthesis and characterization of the ligands and the Ir(III) complexes

2-(1-naphthyl)benzothiazole (nbt): 2-aminothiophenol (3 g, 23.96 mmol) and 1-naphthaldehyde (3.6 g, 23.05 mmol) were refluxed in DMSO (25 mL) under nitrogen atmosphere at 195 °C for 3 h. After cooling, a small quantity of water was added. The mixture was extracted with dichloromethane (3 × 100 mL), and the combined organic phase was dried over anhydrous $MgSO_4$. After filtering, the filtrate was evaporated to dryness under reduced pressure. The crude was purified by chromatography on silica gel using petroleum ether/ethyl acetate (15:1, v/v) as the eluent to give yellow powdery 2-(1-naphthyl)benzothiazole (4.82 g, 80%). ^1H NMR (400 MHz, $CDCl_3$, δ, ppm): 8.93 (d, $J = 8.8$ Hz, 1H), 8.21 (d, $J = 8.0$ Hz, 1H), 7.98 (t, $J = 8.0$ Hz, 2H), 7.94 (d, $J = 8.0$ Hz, 2H), 7.63 (t, $J = 7.4$ Hz, 1H), 7.61–7.54 (m, 3H), 7.45 (t, $J = 7.6$ Hz, 1H).

$(nbt)_2Ir(\mu\text{-}Cl)_2Ir(nbt)_2$: The cyclometalated Ir(III) μ-chloro-bridged dimer of $(nbt)_2Ir(\mu\text{-}Cl)_2Ir(nbt)_2$ was synthesized by refluxing $IrCl_3 \cdot nH_2O$ (2.00 g, 6.24 mmol) with 2.5 equiv. of 2-(1-naphthyl)benzothiazole (4.06 g, 15.54 mmol) in a 3:1 mixture of 2-ethoxyethanol and water (48 mL) under nitrogen at 135 °C for 24 h. The mixture was cooled to room temperature, and 100 mL of water was added. The rufous precipitate was collected by filtration, and washed twice with water and then methanol/water mixture (1:2, v/v). The solid was pumped dry to give the crude dimer of 5.35 g. The crude dimer was directly used for subsequent preparation of the Ir(III) complexes.

$(nbt)_2Ir(pic)$: The chloro-bridged dimer complex (0.80 g, 0.534 mmol), picolinic acid (0.27 g, 2.19 mmol) and sodium carbonate (2.10 g, 19.80 mmol) were refluxed in 2-ethoxyethanol (50 mL) under nitrogen atmosphere at 95 °C for 24 h. After cooling, a small quantity of water was added. The mixture was extracted with dichloromethane (50 mL × 3). The organic phase was dried over anhydrous $MgSO_4$. After filtering, the filtrate was evaporated to dryness under reduced pressure. The crude was purified by chromatography on silica gel using dichloromethane/ethyl acetate (10:1, v/v) as the eluent to give deep red powdery $(nbt)_2Ir(pic)$ in 80.66% yield (0.72 g). ^1H NMR (400 MHz, $CDCl_3$, δ, ppm): 8.64 (d, 1H, $J = 8.0$ Hz, Aryl-H), 8.57 (t, 2H, $J = 8.0$ Hz, Aryl-H), 8.17 (d, 1H, $J = 8.0$ Hz, Aryl-H), 7.95 (dd, 2H, $J = 8.0$ Hz, Aryl-H), 7.86 (dd, 2H, $J = 5.2$ Hz, $J = 7.6$ Hz, Aryl-H), 7.74 (d, 1H, $J = 8.0$ Hz, Aryl-H), 7.69–7.57 (m, 3H, Aryl-H), 7.51–7.42 (m, 3H, Aryl-H), 7.34 (t, 3H, $J = 8.4$ Hz, Aryl-H), 7.15 (d, 1H, $J = 8.8$ Hz, Aryl-H), 7.10 (d, 1H, $J = 8.4$ Hz, Aryl-H), 6.98 (t, 1H, $J = 8.0$ Hz, Aryl-H), 6.83 (d, 1H, $J = 8.4$ Hz, Aryl-H), 6.42 (d, 1H, $J = 8.4$ Hz, Aryl-H), 6.24 (d, 1H, $J = 8.4$ Hz, Aryl-H). MS: Calcd for $C_{40}H_{24}IrN_3O_2S_2$, 834.98; Found, 835.67.

$(nbt)_2Ir(pic\text{-}OH)$: A mixture of the chloro-bridged dimer complex (2.00 g, 1.34 mmol), 3-hydroxypicolinic acid (0.56 g, 4.03 mmol) and sodium carbonate (3.55 g, 33.49 mmol) in 2-ethoxyethanol (60 mL) was refluxed under N_2 atmosphere for 24 h. After cooling to room temperature, the solvent was evaporated in vacuum and dissolved in dichloromethane (150 mL). The organic phase was washed with water and dried over anhydrous $MgSO_4$. The solvent was evaporated to give the crude product, which was purified by chromatography on silica gel using dichloromethane/ethyl acetate/methanol (13:1:0.5, v/v/v) as the eluent to provide deep red product $(nbt)_2Ir(pic\text{-}OH)$ (1.94 g, 85.3%). ^1H NMR (400 MHz, $CDCl_3$, δ, ppm): 13.51 (s, 1H, -OH), 8.60 (dd, 2H, $J = 8.0$ Hz, $J = 8.4$ Hz, Aryl-H), 8.45 (d, 1H, $J = 8.0$ Hz, Aryl-H), 7.98 (t, 2H, $J = 8.4$ Hz, Aryl-H), 7.73 (d, 1H, $J = 7.6$ Hz, Aryl-H), 7.69–7.58 (m, 3H, Aryl-H), 7.53–7.42 (m, 3H, Aryl-H), 7.39–7.33 (m, 4H, Aryl-H), 7.19–7.04 (m, 4H, Aryl-H), 6.77 (d, 1H, $J = 8.6$ Hz, Aryl-H), 6.42 (d, 1H, $J = 7.2$ Hz, Aryl-H), 6.33 (d, 1H, $J = 8.0$ Hz, Aryl-H). MS: Calcd for $C_{40}H_{24}IrN_3O_3S_2$, 850.98; Found, 851.81.

$(nbt)_2Ir(pic\text{-}Cz)$: To a solution of $(nbt)_2Ir(pic\text{-}OH)$ (1.50 g, 1.76 mmol) in acetone (80 mL) were added 9-(4-(bromomethyl) phenyl)-9*H*-carbazole (0.75 g, 2.22 mmol) and Cs_2CO_3 (0.72 g, 2.21 mmol). The reaction mixture was refluxed under N_2 atmosphere for 24 h. After cooling to room temperature, the solvent was evaporated in vacuum and dissolved in dichloromethane (150 mL). The organic phase was washed with water and dried over anhydrous Na_2SO_4. The solvent was evaporated to give the crude product, which was applied to column chromatography on silica gel, eluting with ethyl acetate/petroleum ether (1:3, v/v) to provide the product (0.82 g, 42.1%). ^1H NMR (400 MHz, $CDCl_3$, δ, ppm): 8.72 (d, 1H, $J = 8.0$ Hz, Aryl-H), 8.64 (d, 1H, $J = 8.8$ Hz, Aryl-H), 8.57 (d, 1H, $J = 8.4$ Hz, Aryl-H), 8.14 (d, 2H, $J = 7.6$ Hz, Aryl-H), 7.97 (d, 1H, $J = 8.0$ Hz, Aryl-H), 7.91 (d, 1H, $J = 8.0$ Hz, Aryl-H), 7.73 (d, 1H, $J = 8.0$ Hz, Aryl-H), 7.68 (d, 1H, $J = 7.2$ Hz, Aryl-H), 7.64–7.59 (m, 6H, Aryl-H), 7.54 (dd, 2H, $J = 7.2$ Hz, Aryl-H), 7.47–7.38 (m, 12H), 7.13 (d, 1H, $J = 8.4$ Hz, Aryl-H), 7.08 (d, 1H, $J = 8.4$ Hz, Aryl-H), 6.99 (t, 1H, $J = 7.6$ Hz, Aryl-H), 6.79 (d, 1H, $J = 8.4$ Hz, Aryl-H), 6.40 (d, 1H, $J = 8.4$ Hz, Aryl-H), 6.29 (d, 1H, $J = 8.8$ Hz, Aryl-H), 5.35 (s, 2H, Ar-O–CH_2–). MS: Calcd for $C_{59}H_{37}IrN_4O_3S_2$, 1106.30; Found, 1107.20.

$(nbt)_2Ir(pic\text{-}Ox)$: The preparation of $(nbt)_2Ir(pic\text{-}Ox)$ was similar to that described for $(nbt)_2Ir(pic\text{-}Cz)$, which was obtained from $(nbt)_2Ir(pic\text{-}OH)$ (1.138 g, 1.33 mmol) and 2-[4-(Bromomethyl) phenyl]-5-(4-tertbutylphenyl)-1,3,4-oxadiazole (0.614 g, 1.66 mmol) in the presence of anhydrous Cs_2CO_3 (0.541 g, 1.66 mmol). The crude was purified by chromatography on silica gel using dichloromethane/ethyl acetate (10:1, v/v) as the eluent to give the product (0.71 g, 46.5%). ^1H NMR (400 MHz, $CDCl_3$, δ, ppm): 8.71 (d, 1H, $J = 8.0$ Hz, Aryl-H), 8.62 (d, 1H, $J = 8.4$ Hz, Aryl-H), 8.58 (d, 1H, $J = 8.8$ Hz, Aryl-H), 8.07–7.94 (m, 2H, Aryl-H), 7.72 (d, 1H, $J = 8.0$ Hz, Aryl-H), 7.67–7.61 (m, 3H, Aryl-H), 7.59–7.53 (m, 7H, Aryl-H), 7.48 (t, 1H, $J = 7.2$ Hz, Aryl-H), 7.42 (t, 1H, $J = 7.2$ Hz, Aryl-H), 7.38–7.31 (m, 4H, Aryl-H), 7.16–7.08 (m, 2H, Aryl-H), 6.95 (t, 1H, $J = 7.6$ Hz, Aryl-H), 6.77 (d, 1H, $J = 8.4$ Hz, Aryl-H), 6.40 (d, 1H, $J = 8.4$ Hz, Aryl-H), 6.25 (d, 1H, $J = 8.8$ Hz, Aryl-H), 5.32 (s, 2H, Ar-O–CH_2–), 1.38 (s, 12H, –CH_3). MS: Calcd for $C_{59}H_{42}IrN_5O_4S_2$, 1141.34; Found, 1142.24.

2.3. Crystallography

The diffraction data of the cyclometalated ligand 2-(1-naphthyl) benzothiazole (nbt) were collected with a Bruker Smart Apex CCD area detector with graphite-monochromatized Mo-Kα radiation (λ = 0.71073 Å) at 188(2) K. The structure was solved by using the program SHELXL and Fourier difference techniques, and refined by full-matrix least-squares method on F^2. All hydrogen atoms were added theoretically.

2.4. OLEDs fabrication and characterization

The multilayer OLEDs with a device architecture of ITO/TAPC (20 nm)/CBP:Ir(III) complex (x wt%, 50 nm)/TPBi (50 nm)/Liq (2 nm)/Al (150 nm) were fabricated by vacuum-deposition method. All organic layers were sequentially deposited without breaking vacuum (2×10^{-5} Pa). Thermal deposition rates for organic materials and Al were ~2 Å/s and 10 Å/s, respectively. The active area of the devices was 12 mm^2. A cathode consisting of an ultrathin Liq interfacial layer with a nominal thickness of 2 nm and an Al layer ca. 150 nm thick was deposited by thermal evaporation. The deposition rates for Liq and Al were ~1 and 10 Å s^{-1}, respectively. The EL spectra and Commission Internationale de L'Eclairage (CIE) coordinates were measured on a Hitachi MPF-4 fluorescence spectrometer. The characterization of brightness-current-voltage (B–I–V) were measured with a 3645 DC power supply combined with a 1980A spot photometer and were recorded simultaneously. All measurements were done in the air at room temperature without any encapsulation.

3. Results and discussion

3.1. Synthesis and characterization of the Ir(III) complexes

The synthesis of the phosphorescent Ir(III) complexes from Scheme 1 began first with preparing the cyclometalated ligand 2-(1-naphthyl)benzothiazole (nbt). The cyclometalated ligand nbt was successfully synthesized via reacting 2-aminothiophenol with 1-naphthaldehyde at 195 °C in DMSO solvent. This method leads to higher yield of the target product (80%). The chlorobridged dimer complex $(nbt)_2Ir(\mu\text{-}Cl)_2Ir(nbt)_2$ was synthesized from nbt and $IrCl_3 \cdot nH_2O$ in a refluxing 2-ethoxyethanol/water mixture. The complexes $(nbt)_2$Ir(pic-Cz) and $(nbt)_2$Ir(pic-Ox) were obtained by two steps. First, the intermediate $(nbt)_2$Ir(pic-OH) was synthesized by reacting the chlorobridged dimer with 3-hydroxypicolinic acid. Then the intermediate $(nbt)_2$Ir(pic-OH) was reacted with 2-[4-(Bromomethyl)phenyl]-5-(4-tertbutylphenyl)-1,3,4-oxadiazole or 9-(4-(bromomethyl)phenyl)-9*H*-carbazole in acetone to get $(nbt)_2$Ir(pic-Ox) or $(nbt)_2$Ir(pic-Cz). Details are described in the Experimental section.

The cyclometalated ligand nbt was characterized by X-ray diffraction. Suitable crystal of the ligand nbt was obtained by the evaporation of its methanol solution. The crystal structure and packing diagram of nbt is given in Fig. 1. The crystal of nbt belongs to the orthorhombic space group P2(1)2(1)2(1), $a = 7.9994(7)$ Å, $b = 12.0871(10)$ Å, $c = 13.0874(11)$ Å, $\alpha = \beta = \gamma = 90°$, $U = 1265.41(19)$ Å^3, $Z = 4$, $Dc = 1.372$ g cm^{-3}, $\mu = 0.238$ mm^{-1}. As shown in Fig. 2, the N(1)–C(1) bond length (1.299(2) Å) is shorter than the N(1)–C(2) bond length (1.391(2) Å), which has the C=C characteristic. The S(1)–C(1), S(1)–C(7) and C(1)–C(8) bond lengths are 1.758(18), 1.733(19) and 1.478(2) Å, respectively. The benzothiazole moiety and naphthyl ring are not in a coplane, and the dihedral angel between of them is 48.90°. From the packing diagram of nbt, there are four nbt molecules in a unit cell, and there is no inter- or inner-molecular π-π stacking interaction in the crystal lattice.

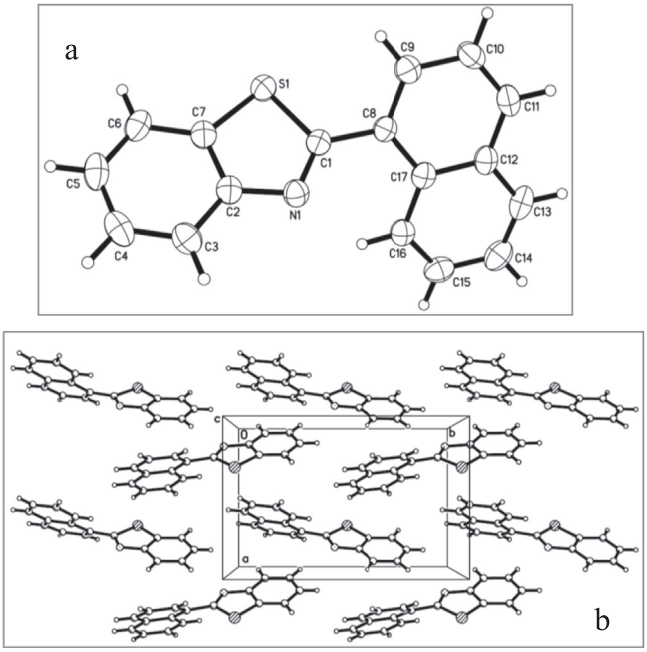

Fig. 1. Crystal structure (a) and packing diagram (b) of 2-(1-naphthyl)benzothiazole (nbt).

3.2. Photophysical, electrochemical and thermal properties of the Ir(III) complexes

Fig. 2 shows the UV–vis absorption and photoluminescence spectra of $(nbt)_2$Ir(pic-Ox) and $(nbt)_2$Ir(pic-Cz) in diluted dichloromethane solutions. Seven absorption bands at 245, 282, 292, 346, 435, 491 and 524 nm were observed in the absorption spectra of $(nbt)_2$Ir(pic-Ox) and $(nbt)_2$Ir(pic-Cz). The absorption bands at $\lambda < 400$ nm are assigned to the spin-allowed $^1(\pi \rightarrow \pi^*)$ transitions of the ligands in the complex. The bands at the longer wavelength (435, 491 and 524 nm) can be assigned to both spin-orbit coupling enhanced $^3(\pi \rightarrow \pi^*)$ and spin-forbidden metal-to-ligand charge transfer ^{3}MLCT (metal-ligand-charge-transfer) transitions [33–35].

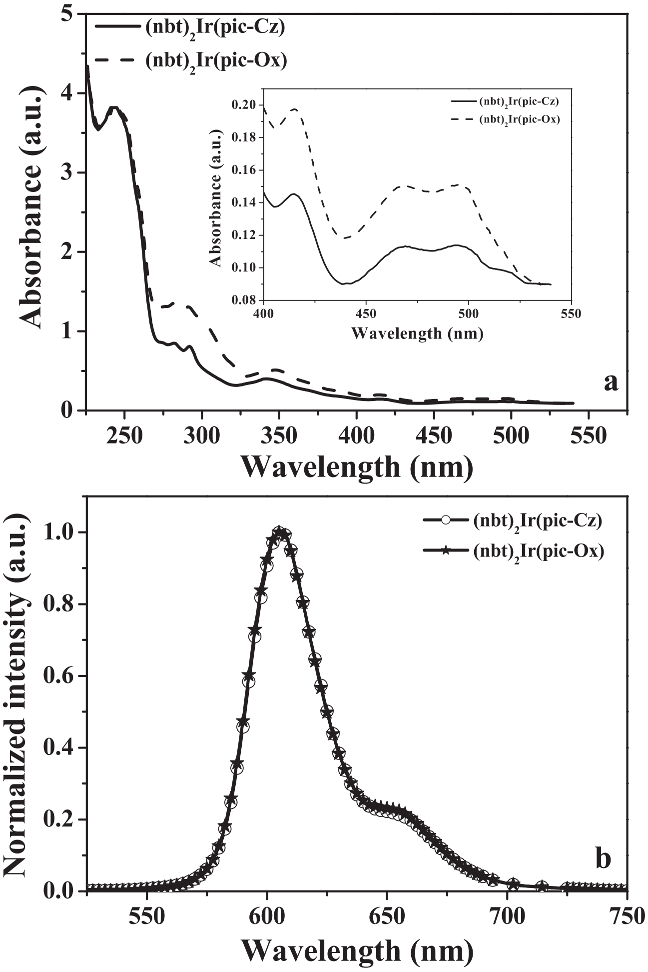

Fig. 2. The UV–vis absorption spectra (a) and photoluminescence spectra (b) of the Ir(III) complexes.

As shown in Fig. 2, the photoluminescence spectra of (nbt)$_2$Ir(pic-Ox) and (nbt)$_2$Ir(pic-Cz) in dichloromethane solutions greatly resemble each other, these complexes all exhibit red emissions with a maximum main peak (605 nm) and a shoulder peak (655 nm). The Commission Internationale de L'Eclairage (CIE) coordinates is (0.65, 0.35).

The luminescence quantum yields of the Ir(III) complexes in the solid states were measured in order to study their optical characteristics. The quantum yields of (nbt)$_2$Ir(pic-Cz) and (nbt)$_2$Ir(pic-Ox) at room temperature were measured to be 2.08% and 2.40% and in the solid states by an absolute method using the Edinburgh Instruments (FLS920) integrating sphere excited at 380 nm with the Xe lamp. The result indicates that the luminescence quantum yields of the Ir(III) complex containing the hole transporting group-functionalized picolinate ligand was greater than that of the complex with the electron transporting group-functionalized picolinate ligand.

Cyclic voltammetry (CV) was employed to investigate the electrochemical behavior of these Ir(III) complexes. The Ir(III) complexes were dissolved in dichloromethane with tetra-*n*-butylammonium tetrafluoroborate (0.1 mol/L) as the electrolyte. A platinum working electrode and a saturated Ag/AgCl reference electrode were used. Ferrocene was used for potential calibration. The highest occupied molecular orbital (HOMO) and the lowest unoccupied molecular orbital (LUMO) energy levels of these Ir(III) complexes were calculated from their cyclic voltammetry measurements and their absorption spectra. The cyclic voltammograms of ferrocene and these Ir(III) complexes are shown in Fig. 3. The potentials for oxidation of the complexes were observed to be 0.86 V. At the same condition, the oxidation peak and the reductive peak of ferrocene were observed at 0.51 and 0.37 V, respectively, then the $E_{1/2}$ (Fc/Fc$^+$) is 0.44 V. Thus the HOMO energy levels of the Ir(III) complexes were determined to be −5.22 V regarding the energy level of ferrocene/ferrocenium as −4.80 eV [36]. The optical band edge of the Ir(III) complexes were estimated to be about 561 nm, which corresponds to 2.21 eV. Then the LUMO energy levels of (nbt)$_2$Ir(pic-Cz) and (nbt)$_2$Ir(pic-Ox) are calculated to be −3.01 eV.

The thermogravimetric analyses (TGA) were performed in flowing drying nitrogen atmosphere at the heating rate of 10 °C/min. The result of TGA measurements of the Ir(III) complexes are shown in Fig. 4. The complexes (nbt)$_2$Ir(pic-Cz) and (nbt)$_2$Ir(pic-Ox) have good thermal stability before 285 °C, the complexes (nbt)$_2$Ir(pic-Cz) and (nbt)$_2$Ir(pic-Ox) begin to decompose at 285 °C accompanied by the weight losses. At 295 and 386 °C, the TGA curve of the complex (nbt)$_2$Ir(pic-Cz) shows two sharp weight losses. At 295, 378 and 441 °C, the TGA curve of the complex (nbt)$_2$Ir(pic-Ox) shows three sharp weight losses. From the thermogravimetric analyses of the Ir(III) complexes, the complexes meet with the thermal stability requirement of fabrication of OLED luminescence application.

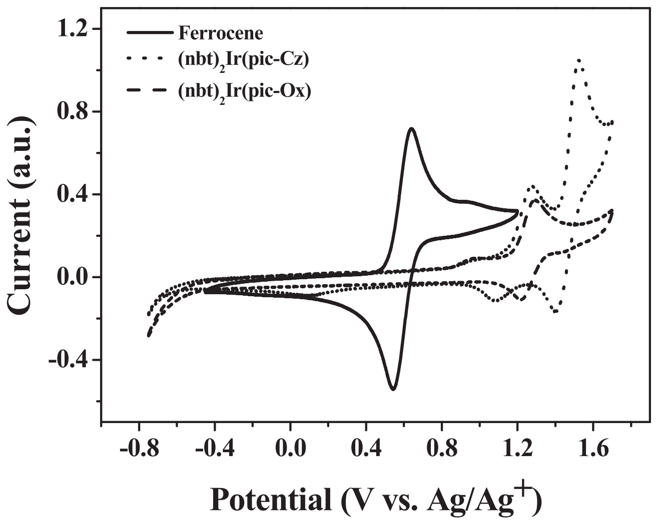

Fig. 3. Cyclic voltammograms of ferrocene and the Ir(III) complexes.

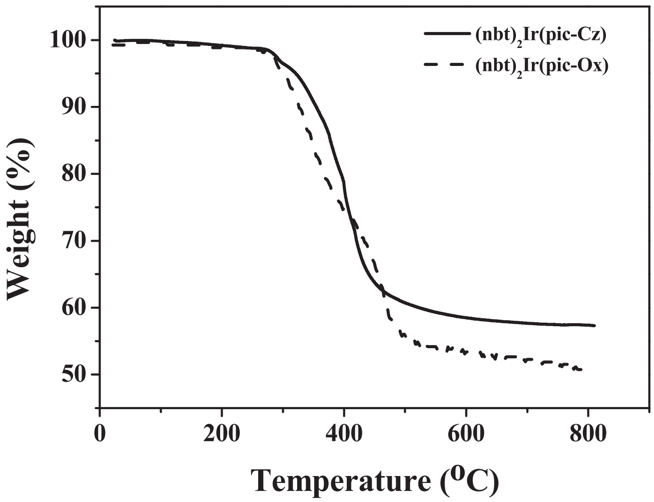

Fig. 4. Thermogravimetric analyses (TGA) of the Ir(III) complexes.

Table 1 summarizes the photophysical, thermal and electrochemical properties of (nbt)$_2$Ir(pic-Cz) and (nbt)$_2$Ir(pic-Ox).

3.3. OLEDs performances of the Ir(III) complexes

The devices based on the Ir(III) complexes with a device architecture of ITO/TAPC (20 nm)/CBP:Ir(III) complex (x wt%, 50 nm)/TPBi (50 nm)/Liq (2 nm)/Al (150 nm) were fabricated by vacuum-deposition method. The emitting layers were consisted of host materials CBP and dopant of the complexes (nbt)$_2$Ir(pic-Cz) and (nbt)$_2$Ir(pic-Ox) at different concentrations (x wt%). TAPC and TPBi were used as hole transport and electron transport materials, respectively. Liq was used as the electron-injection layer. In the case, the doped concentrations of the Ir(III) complexes were about 8 wt%, 10 wt%, 15 wt% and 20 wt%, respectively.

The doped devices of (nbt)$_2$Ir(pic-Cz) and (nbt)$_2$Ir(pic-Ox) exhibit red emissions with a maximum main peak at 605 nm and a shoulder peak at 655 nm, the EL spectra of (nbt)$_2$Ir(pic-Cz) and (nbt)$_2$Ir(pic-Ox) resemble closely their PL spectra in dichloromethane solutions, and the EL spectra of the devices were independent of the different dopant concentrations and at different driving voltages. The Commission Internationale de L'Eclairage (CIE) coordinates of the devices were (0.65, 0.33).

The luminance *vs.* the driving voltage and the current efficiency *vs.* the driving voltage characteristics of the devices fabricated from (nbt)$_2$Ir(pic-Cz) and (nbt)$_2$Ir(pic-Ox) are shown in Figs. 5 and 6, respectively. Table 2 summarized the performances of the devices based on (nbt)$_2$Ir(pic-Cz) and (nbt)$_2$Ir(pic-Ox). In the devices fabricated from (nbt)$_2$Ir(pic-Cz), the maximum brightness of 2830, 3074, 2685 and 1965 cd/m^2 were observed in the devices with 8 wt%, 10 wt%, 15 wt% and 20 wt% doping concentrations, respectively. The maximum luminous efficiencies of 4.03, 4.84, 3.71 and 3.53 cd/A were obtained in the devices with different doping concentrations. By comparing the device performances of the different doping concentrations, the devices based on (nbt)$_2$Ir(pic-Cz) with

Table 1
Photophysical, thermal and electrochemical properties of the Ir(III) complexes.

Complexes	UV–vis (nm)	PL (nm)	T_d (°C)	Φ_f (%)	E_{OX} (V)	HOMO (eV)	LUMO (eV)
$(nbt)_2Ir(pic\text{-}Cz)$	245, 282, 292, 346, 435, 491, 524	605, 655	285	2.40	0.86	−5.22	−3.01
$(nbt)_2Ir(pic\text{-}Ox)$	245, 282, 292, 346, 435, 491, 524	605, 655	285	2.08	0.86	−5.22	−3.01

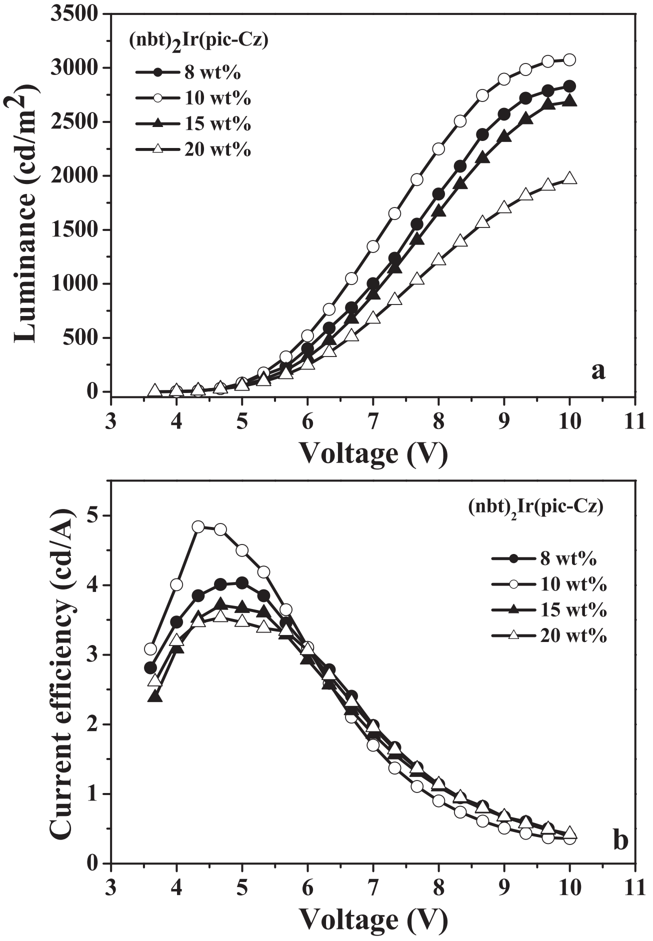

Fig. 5. The luminance vs. voltage (a) and current efficiency vs. voltage (b) curves of the devices with different $(nbt)_2Ir(pic\text{-}Cz)$ concentrations.

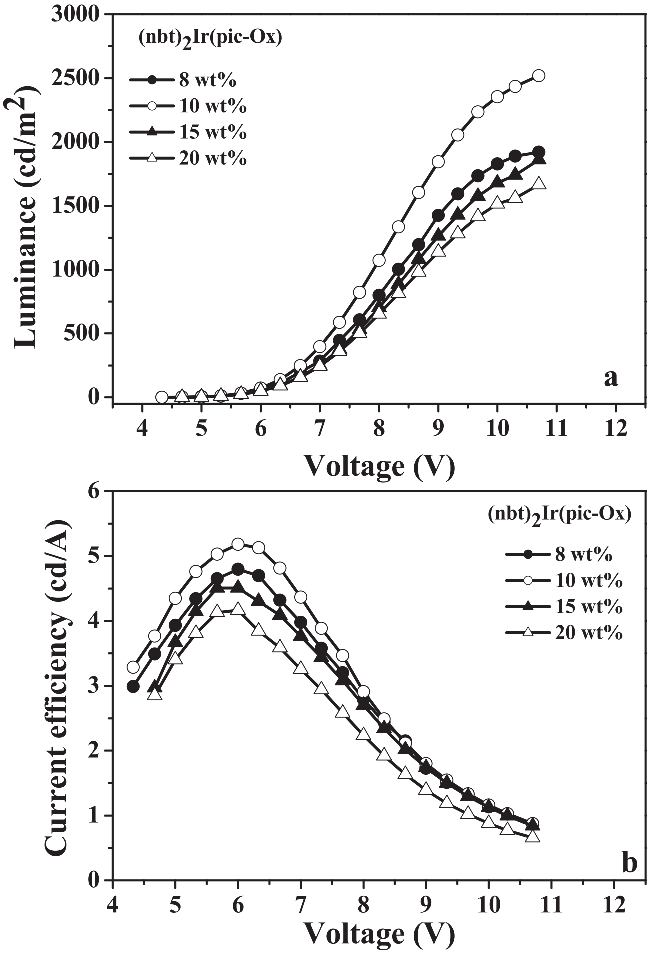

Fig. 6. The luminance vs. voltage (a) and current efficiency vs. voltage (b) curves of the devices with different $(nbt)_2Ir(pic\text{-}Ox)$ concentrations.

Table 2
EL performances of the Ir(III) complexes.

Complexes	Concentration	L_{max} (cd/m^2)	LE_{max} (cd/A)
$(nbt)_2Ir(pic)$	8 wt%	1322@16 V	2.78@6.1 V
	10 wt%	1345@16 V	2.96@6.1 V
	12 wt%	1432@16 V	3.79@6.1 V
	15 wt%	1147@16 V	3.16@6.1 V
$(nbt)_2Ir(pic\text{-}Cz)$	8 wt%	2830@10 V	4.03@5.0 V
	10 wt%	3074@10 V	4.84@4.7 V
	15 wt%	2685@10 V	3.71@4.7 V
	20 wt%	1965@10 V	3.53@4.7 V
$(nbt)_2Ir(pic\text{-}Ox)$	8 wt%	1921@10.7 V	4.80@6.0 V
	10 wt%	2520@10.7 V	5.18@6.0 V
	15 wt%	1860@10.7 V	4.51@6.0 V
	20 wt%	1665@10.7 V	4.16@6.0 V

10 wt% doping concentration showed the best EL performance. The maximum current efficiency of 4.84 cd/A at 4.67 V and maximum brightness of 3074 cd/m^2 at 10.7 V have been observed in the device. When the doping concentration is over 10 wt%, the current efficiency and the brightness at a given driving voltage decrease. For the complex $(nbt)_2Ir(pic\text{-}Ox)$, the device with 10 wt% doping concentration exhibited the best EL performance. The device had a maximum brightness of 2520 cd/m^2 at 10.7 V and a maximum current efficiency of 5.18 cd/A at 6 V.

To compare the performance of the devices based on $(nbt)_2Ir(pic\text{-}Cz)$ and $(nbt)_2Ir(pic\text{-}Ox)$, the devices based on the complex $(nbt)_2Ir(pic)$ without the carbazole or oxadiazole units as a reference material were fabricated in the same device architecture. The doped devices of $(nbt)_2Ir(pic)$ also exhibit red emissions with a maximum main peak at 605 nm and a shoulder peak at 655 nm. The luminance *vs.* the driving voltage and the current efficiency *vs.* the driving voltage characteristics of the devices fabricated with different $(nbt)_2Ir(pic)$ doping concentrations are shown in Fig. 7. At a voltage of 16 V, the maximum brightness of 1322, 1345, 1432 and 1147 cd/m^2 were observed in the devices with 8, 10, 12 and 15 wt% doping concentrations, respectively. The maximum luminous efficiencies of 2.78, 2.96, 3.79 and 3.16 cd/A were obtained in the

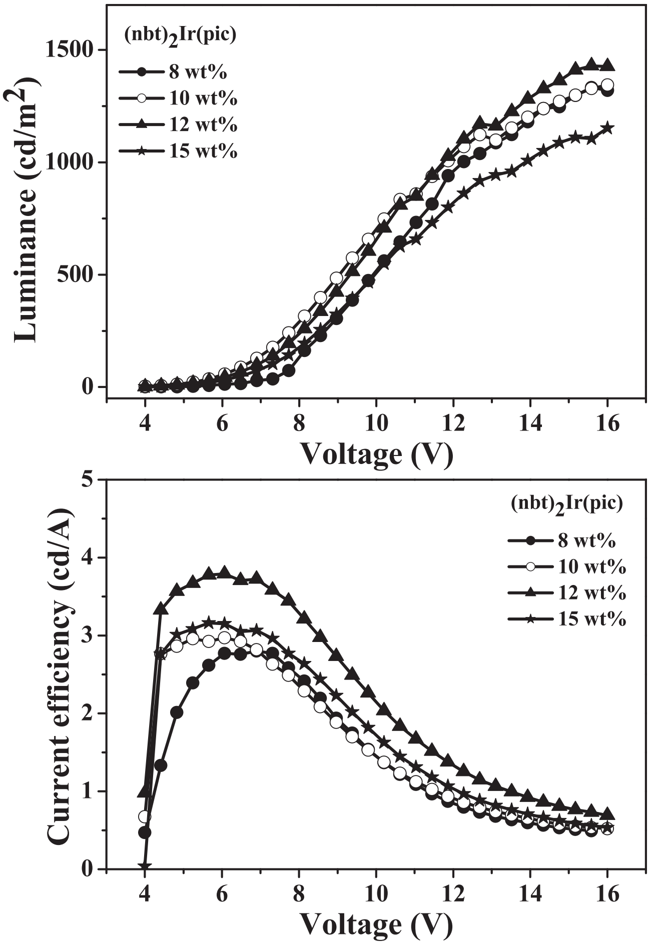

Fig. 7. The luminance vs. voltage (a) and current efficiency vs. voltage (b) curves of the devices with different the reference material $(nbt)_2Ir(pic)$ concentrations.

devices with different doping concentrations at 6.1 V. By comparing the performance of different doping concentrations, the device with 12 wt% doping concentration showed the best EL efficiency performance. The maximum current efficiency of 3.79 cd/A and maximum brightness of 1432 cd/m^2 have been observed in the device.

As shown in Table 2, the EL performances of the Ir(III) complexes were obviously influenced by the ancillary ligands. Because of the better carrier-injection and carrier-transportation balance due to the incorporation of an electron-transporting moiety on the Ir(III) complex $(nbt)_2Ir(pic\text{-}Ox)$, the devices fabricated from $(nbt)_2Ir(pic\text{-}Ox)$ complex display higher current efficiency in contrast with the devices based on $(nbt)_2Ir(pic\text{-}Cz)$. When an electron-transporting group of diaryl-1,3,4-oxadiazole moiety is incorporated, the charge carrier injection balance in the devices is improved, resulting in the effective carrier recombination, consequently, leading to the improvement of the device performances.

4. Conclusion

We reported the synthesis, photophysics, electrochemical characterization and thermal stabilities of two new iridium(III) complexes with the carrier transporting group-functionalized picolinate as the ancillary ligands and 2-(1-naphthyl)benzothiazole as the cyclometalated ligand. The Ir(III) complexes have higher thermal stability, and exhibit red emission with a maximum main peak at 605 nm and a shoulder peak at 655 nm. The EL devices based on the Ir(III) complexes were fabricated by the evaporation method. When the doping concentration is 10 wt%, the light-emitting devices fabricated by $(nbt)_2Ir(pic\text{-}Cz)$ and $(nbt)_2Ir(pic\text{-}Ox)$ exhibited red emissions with a maximum brightness of 3074 and 2520 cd/m^2 at 10.7 V and a maximum current efficiency of 4.84 and 5.18 cd/A, respectively.

Acknowledgements

This work was supported by the National Natural Science Foundation of China (Grant 61166003), and also supported by the Program for Changjiang Scholars and Innovative Research Team in University (IRT0629).

Supplementary material

CCDC 945231 contains the supplementary crystallographic data for the ligand 2-(1-naphthyl)benzothiazole (nbt) in this paper. The data can be obtained free of charge via http://www.ccdc.cam.ac.uk/conts/retrieving.html, or from the Cambridge Crystallographic Data Centre, 12 Union Road, Cambridge CB2 1EZ, UK; fax: (+44) 1223-336-033; or e-mail: deposit@ccdc.cam.ac.uk.

References

[1] (a) M.A. Baldo, M.E. Thompson, S.R. Forrest, High-efficiency fluorescent organic light-emitting devices using a phosphorescent sensitizer, Nature 403 (2000) 750–753;
(b) X.L. Yang, G.J. Zhou, W.-Y. Wong, Functionalization of phosphorescent emitters and their host materials by main-group elements for phosphorescent organic light-emitting devices, Chem. Soc. Rev. 44 (2015) 8484–8575;
(c) W.-Y. Wong, C.-L. Ho, Functional metallophosphors for effective charge carrier injection/transport: new robust OLED materials with emerging applications, J. Mater. Chem. 19 (2009) 4457–4482;
(d) W.-Y. Wong, C.-L. Ho, Heavy metal organometallic electrophosphors derived from multi-component chromophores, Coord. Chem. Rev. 253 (2009) 1709–1758;
(e) G. Zhou, W.Y. Wong, S. Suo, Recent progress and current challenges in phosphorescent white organic light-emitting diodes (WOLEDs), J. Photochem. Photobio. C. Photochem. Rev. 11 (2010) 133–156.

[2] (a) M.A. Baldo, M.E. Thompson, S.R. Forest, Phosphorescent materials for application to organic light emitting devices, Pure Appl. Chem. 71 (1999) 2095–2106;
(b) C.-L. Ho, W.-Y. Wong, Small-molecular blue phosphorescent dyes for organic light-emitting devices, New J. Chem. 37 (2013) 1665–1683;
(c) X.B. Xu, X.L. Yang, J. Zhao, G.J. Zhou, W.-Y. Wong, Recent advances in solution-processable dendrimers for highly efficient phosphorescent organic light-emitting diodes (PHOLEDs), Asian J. Org. Chem. 4 (2015) 394–429.

[3] (a) P.T. Furuta, L. Deng, S. Garon, M.E. Thompson, J.M.J. Frechet, Platinum-functionalized random copolymers for use in solution-processible, efficient, near-white organic light-emitting diodes, J. Am. Chem. Soc. 126 (2004) 15388–15389;
(b) G.J. Zhou, W.-Y. Wong, X.L. Yang, New design tactics in OLEDs using functionalized 2-phenylpyridine-type cyclometalates of iridium(III) and platinum(II), Chem. Asian J. 6 (2011) 1706–1727;
(c) L. Ying, C.-L. Ho, H.B. Wu, Y. Cao, W.-Y. Wong, White polymer light-emitting devices for solid-state lighting: materials, devices, and recent progress, Adv. Mater. 26 (2014) 2459–2473;
(d) X.L. Yang, G.J. Zhou, W.-Y. Wong, Recent design tactics for high performance white polymer light-emitting diodes, J. Mater. Chem. C 2 (2014) 1760–1778;
(e) C.-L. Ho, H. Li, W.-Y. Wong, Red to near-infrared organometallic phosphorescent dyes for OLED applications, J. Organomet. Chem. 751 (2014) 261–285.

[4] M. Thompson, The evolution of organometallic complexes in organic light-emitting devices, MRS Bull. 32 (2007) 694–701.

[5] X. Gong, J.C. Ostrowski, G.C. Bazan, A.J. Heeger, M.S. Liu, A.K.Y. Jen, Electrophosphorescence from a conjugated copolymer doped with an iridium complex: high brightness and improved operational stability, Adv. Mater. 15 (2003) 45–49.

[6] P.-T. Chou, Y. Chi, Phosphorescent dyes for organic light-emitting diodes, Chem. Eur. J. 13 (2007) 380–395.

[7] W.S. Huang, C.W. Lin, J.T. Lin, J.S. Huang, C.W. Chu, Y.H. Wu, H.C. Lin, Highly branched green phosphorescent tris-cyclometalated iridium(III) complexes for solution-processed organic light-emitting diodes, Org. Electron. 10 (2009) 594–606.

[8] (a) W.-Y. Wong, C.-L. Ho, Heavy metal organometallic electrophosphors derived from multi-component chromophores, Coord. Chem. Rev. 253 (2009) 1709–1758;
(b) C.-L. Ho, B. Yao, B.H. Zhang, K.-L. Wong, W.-Y. Wong, Z.Y. Xie, L.X. Wang, Z.Y. Lin, Metallophosphors of iridium(III) containing borylated oligothiophenes with electroluminescence down to the near-infrared region, J. Organomet. Chem. 730 (2013) 144–155.
[9] Y. Chi, P.-T. Chou, Transition-metal phosphors with cyclometalating ligands: fundamentals and applications, Chem. Soc. Rev. 39 (2010) 638–655.
[10] L.X. Xiao, Z.J. Chen, B. Qu, J.X. Luo, S. Kong, Q.H. Gong, J. Kido, Recent progresses on materials for electrophosphorescent organic light-emitting devices, Adv. Mater. 23 (2011) 926–952.
[11] G.J. Zhou, W.-Y. Wong, B. Yao, Z.Y. Xie, L.X. Wang, Triphenylamine-dendronized pure red iridium phosphors with superior OLED efficiency/color purity trade-offs, Angew. Chem. Int. Ed. 46 (2007) 1149–1151.
[12] T.Z. Yu, Y.L. Shi, H.F. Chai, L.X. Niu, P. Liu, Y.L. Zhao, J.D. Kang, B. Gao, H. Zhang, Synthesis, characterization, and photo- and electro-luminescence of Ir(III) complexes containing carrier transporting group-substituted β-diketonate ligand, RSC Adv. 4 (2014) 11680–11688.
[13] T.Z. Yu, Y. Cao, W.M. Su, C.C. Zhang, Y.L. Zhao, D.W. Fan, M.J. Huang, K. Yue, S.Z.D. Cheng, Synthesis, structure, photo- and electro-luminescence of an iridium(III) complex with novel carbazole functionalized β-diketone ligand, RSC Adv. 4 (2014) 554–562.
[14] A. Mori, A. Sekiguchi, K. Masui, T. Shimada, M. Horie, K. Osakada, M. Kawamoto, T. Ikeda, Facile synthesis of 2,5-diarythiazoles via palladium-catalyzed tandem C-H substitutions. Design of tunable light emission and liquid crystalline characteristics, J. Am. Chem. Soc. 125 (2003) 1700–1701.
[15] W.N. Leng, Y.M. Zhou, Q.H. Xu, J.Z. Liu, Synthesis of nonlinear optical polyimides containing benzothiazole moiety and their electro-optical and thermal properties, Polymer 42 (2001) 9253–9259.
[16] P. Hrobárik, I. Sigmundová, P. Zahradník, Preparation of novel push-pull benzothiazole derivatives with reverse polarity: compounds with potential non-linear optic application, Synthesis (2005) 600–604.
[17] R.S. Becker, C. Lenoble, A. Zein, A comprehensive investigation of the photophysics and photochemistry of salicylideneaniline and derivatives of phenylbenzothiazole including solvent effects, J. Phys. Chem. 91 (1987) 3509–3517.
[18] H.Y. Wang, G. Chen, X.P. Xu, H. Chen, S.J. Ji, The synthesis and optical properties of benzothiazole-based derivatives with various π-electron donors as novel bipolar fluorescent compounds, Dyes Pigments 86 (2010) 238–248.
[19] P. Shao, B. Huang, L.Q. Chen, Z.J. Liu, J.G. Qin, H.M. Gong, S. Ding, Q.Q. Wang, Synthesis and two-photon absorption properties of novel heterocycle-based organic molecules, J. Mater. Chem. 15 (2005) 4502–4506.
[20] (a) R.J. Wang, D. Liu, H.C. Ren, T. Zhang, X.Z. Wang, J.Y. Li, Homoleptic tris-cyclometalated iridium complexes with 2-phenylbenzothiazole ligands for highly efficient orange OLEDs, J. Mater. Chem. 21 (2011) 15494–15500;
(b) R.J. Wang, D. Liu, R. Zhang, L.J. Deng, J.Y. Li, Solution-processable iridium complexes for efficient orange-red and white organic light-emitting diodes, J. Mater. Chem. 22 (2012) 1411–1417;
(c) R.J. Wang, D. Liu, H.C. Ren, T. Zhang, H.M. Yin, G.Y. Liu, J.Y. Li, Highly efficient orange and white organic light-emitting diodes based on new orange iridium complexes, Adv. Mater. 23 (2011) 2823–2827.
[21] W.-C. Chang, A.T. Hu, J.-P. Duan, D.K. Rayabarapu, C.-H. Cheng, Color tunable phosphorescent light-emitting diodes based on iridium complexes with substituted 2-phenylbenzothiozoles as the cyclometalated ligands, J. Organomet. Chem. 689 (2004) 4882–4888.
[22] V.K. Rai, M. Nishiura, M. Takimoto, Z.M. Hou, Guanidinate ligated iridium(III) complexes with various cyclometalated ligands: synthesis, structure, and highly efficient electrophosphorescent properties with a wide range of emission colours, J. Mater. Chem. C 1 (2013) 677–689.
[23] I.R. Laskar, S.-F. Hsu, T.-M. Chen, Highly efficient orange-emitting OLEDs based on phosphorescent platinum(II) complexes, Polyhedron 24 (2005) 881–888.
[24] G. Yu, S.W. Yin, Y.Q. Liu, Z.G. Shuai, D.B. Zhu, Structures, electronic states, and electroluminescent properties of a Zinc(II) 2-(2-hydroxyphenyl)benzothiazolate complex, J. Am. Chem. Soc. 125 (2003) 14816–14824.
[25] W.-Y. Wong, X.-Z. Wang, Z. He, A.B. Djurišić, C.-T. Yip, K.-Y. Cheung, H. Wang, C.S.K. Mak, W.-K. Chan, Metallated conjugated polymers as a new avenue towards high-efficiency polymer solar cells, Nat. Mater. 6 (2007) 521–527.
[26] Q.W. Wang, W.-Y. Wong, New low-bandgap polymetallaynes of platinum functionalized with a triphenylamine-benzothiadiazole donor–acceptor unit for solar cell applications, Polym. Chem. 2 (2011) 432–440.
[27] L.F. Lai, J.A. Love, A. Sharenko, J.E. Coughlin, V. Gupta, S. Tretiak, T.-Q. Nguyen, W.-Y. Wong, G.C. Bazan, Topological considerations for the design of molecular donors with multiple absorbing units, J. Am. Chem. Soc. 136 (2014) 5591–5594.
[28] (a) Y. You, S.Y. Park, Phosphorescent iridium(III) complexes: toward high phosphorescence quantum efficiency through ligand control, Dalton Trans. (2009) 1267–1282;
(b) X.L. Yang, X.B. Xu, J.S. Dang, G.J. Zhou, C.-L. Ho, W.-Y. Wong, From mononuclear to dinuclear iridium(III) complex: effective tuning of the optoelectronic characteristics for organic light-emitting diodes, Inorg. Chem. 55 (2016) 1720–1727;
(c) G.J. Zhou, C.-L. Ho, W.-Y. Wong, Q. Wang, D.G. Ma, L.X. Wang, Z.Y. Lin, T.B. Marder, A. Beeby, Manipulating charge-transfer character with electron-withdrawing main-group moieties for the color tuning of iridium electrophosphors, Adv. Funct. Mater. 18 (2008) 499–511;
(d) C.-L. Ho, Q. Wang, C.-S. Lam, W.-Y. Wong, D.G. Ma, L.X. Wang, Z.Q. Gao, C.-H. Chen, K.-W. Cheah, Z.Y. Lin, Phosphorescence color tuning by ligand, and substituent effects of multifunctional iridium(III) cyclometalates with 9-arylcarbazole moieties, Chem. Asian J. 4 (2009) 89–103;
(e) G.J. Zhou, Q. Wang, X.Z. Wang, C.-L. Ho, W.-Y. Wong, D.G. Ma, L.X. Wang, Z.Y. Lin, Metallophosphors of platinum with distinct main-group elements: a versatile approach towards color tuning and white-light emission with superior efficiency/color quality/brightness trade-offs, J. Mater. Chem. 20 (2010) 7472–7484;
(f) C.-L. Ho, L.-C. Chi, W.-Y. Hung, W.-J. Chen, Y.-C. Lin, H. Wu, E. Mondal, G.-J. Zhou, K.-T. Wong, W.-Y. Wong, Carbazole-based coplanar molecule (CmInF) as a universal host for multi-color electrophosphorescent devices, J. Mater. Chem. 22 (2012) 215–224.
[29] G. Hughes, M.R. Bryce, Electron-transporting materials for organic electroluminescent and electrophosphorescent devices, J. Mater. Chem. 15 (2005) 94–107.
[30] A.P. Kulkarni, C.J. Tonzola, A. Batel, S.A. Jenekhe, Electron transport materials for organic light-emitting diodes, Chem. Mater. 16 (2004) 4556–4573.
[31] T.Z. Yu, H.F. Chai, Y.L. Zhao, C.C. Zhang, P. Liu, D.W. Fan, Synthesis, crystal structure and photoluminescence of phosphorescent copper (I) complexes containing hole-transporting carbazole moiety, Spectrochim. Acta A Mol. Biomol. Spectrosc. 109 (2013) 179–185.
[32] T.Z. Yu, J. Meng, Y.L. Zhao, H. Zhang, X.Q. Han, D.W. Fan, Synthesis and rare earth metal ion-sensing properties of aza-crown derivative incorporating with diaryl-1,3,4-oxadiazole, Spectrochim. Acta Part A Mol. Biomol. Spectrosc. 78 (2011) 396–400.
[33] H.H. Rho, G.Y. Park, Y. Ha, Y.S. Kim, Synthesis and photophysical studies of iridium complexes having different ligands, Jpn. J. Appl. Phys. 45 (2006) 568–573.
[34] Z. Bao, A.J. Lovinger, J. Brown, New air-stable n-channel organic thin film transistors, J. Am. Chem. Soc. 120 (1998) 207–208.
[35] Y. Wang, N. Herron, V.V. Grushin, D. LeCloux, V. Petrov, Highly efficient electroluminescent materials based on fluorinated organometallic iridium compounds, Appl. Phys. Lett. 79 (2001) 449–451.
[36] J. Pommerehne, H. Vestweber, W. Guss, R.F. Mahrt, H. Bässler, M. Porsch, J. Daub, Efficient two layer leds on a polymer blend basis, Adv. Mater. 7 (1995) 551–554.